Lesion development is modulated by the natural estrous cycle and mouse strain in a minimally invasive model of endometriosis†

Authors: Dodds, Kelsi N., Beckett, Elizabeth A. H., Evans, Susan F., and Hutchinson, Mark R.

Source: Biology of Reproduction, 97(6) : 810-821

Published By: Society for the Study of Reproduction

URL: https://doi.org/10.1093/biolre/iox132

Biology of Reproduction, 2017, 97(6), 810–821
doi:10.1093/biolre/iox132
Research Article
Advance Access Publication Date: 24 October 2017

OXFORD

Research Article

Lesion development is modulated by the natural estrous cycle and mouse strain in a minimally invasive model of endometriosis†

Kelsi N. Dodds[1,*], Elizabeth A. H. Beckett[1], Susan F. Evans[2] and Mark R. Hutchinson[1,3]

[1]Discipline of Physiology, Adelaide Medical School, University of Adelaide, Adelaide, South Australia, Australia; [2]Discipline of Pharmacology, Adelaide Medical School, University of Adelaide, Adelaide, South Australia, Australia and [3]ARC Centre of Excellence for Nanoscale BioPhotonics, University of Adelaide, Adelaide, South Australia, Australia

*__Correspondence:__ Discipline of Physiology, Adelaide Medical School, University of Adelaide, Frome Road, Adelaide, SA 5005, Australia. Tel: +61-(8)-8313-5117; Fax: +61-(8)-8313-5384; E-mail: kelsi.dodds@adelaide.edu.au

†__Grant Support:__ KND is the recipient of the University of Adelaide Joyner Scholarship in Medicine, an Australian Government Research Training Program Scholarship and a Research Support Grant from the Pelvic Pain Foundation of Australia. SFE also receives support from the Pelvic Pain Foundation of Australia, and MRH is the recipient of an Australian Research Council Fellowship (ID: DP110100297).
Edited by Dr. Haibin Wang, PhD, Xiamen University.

Received 23 August 2017; Revised 10 October 2017; Accepted 19 October 2017

Abstract

Many rodent models of endometriosis are invasive, involving surgery to implant donor endometrial tissue into recipient animals. Moreover, few studies have compared and contrasted lesions between rodent strains and estrous stages without exogenous hormone manipulation. This is despite extensive data demonstrating that genetic and hormonal factors can influence endometriosis progression. Here, we have refined a minimally invasive model of endometriosis using naturally cycling mice (donor and recipient matched for cycle phase) to investigate lesion development in two different strains (C57BL/6 and BALB/c), induced in estrous stages of high and low estrogen (proestrus or estrus, respectively), and with varying amounts of donor endometrial tissue (7.5–40 mg), injected intraperitoneally. The overall probability of developing endometriosis-like lesions was higher in proestrus than estrus, and increased with greater masses of donor tissue. Similarly, the total number of lesions (0–3) increased from 7.5 to 40 mg, and was significantly greater in proestrus C57BL/6 mice but not BALB/cs. The dominant lesion type also differed between mouse strains; C57BL/6 mice were more likely to develop dense-type lesions, whereas BALB/c mice developed a greater proportion of cystic type. These data further support a role for estrogen in the development of endometriosis, and that genetic variance can influence the degree and characteristics of lesions. Our minimally invasive model would be beneficial for studies with outcome measurements particularly sensitive to incisional injury, such as pain, or alterations to sex hormones, including fertility.

Summary Sentence

Incidence and total number of endometriosis-like lesions in mice is greater during periods of higher endogenous estrogen, and lesions display different characteristics between two genetically diverse, wild-type mouse strains (C57BL/6 and BALB/c).

Key words: endometriosis, endometrium, mouse model, mouse strain, estrogen, estrous cycle.

Introduction

Endometriosis is a female-specific chronic inflammatory condition, classically defined as the presence of endometrial-like tissue outside the uterus. Affecting an estimated 10% of women of reproductive age worldwide, endometriosis is highly associated with dysmenorrhea, infertility, and persistent pelvic pain [1]. The mechanistic event underpinning the development of endometriosis lesions is attributed to the flow of menstrual debris through the fallopian tubes to the peritoneal cavity during menses (retrograde menstruation), with the subsequent implantation of endometrial cells [2]. However, this hypothesis cannot fully explain the pathogenesis of endometriosis, as approximately 90% of women aged 15–49 years will exhibit retrograde menstruation [3, 4], yet a much smaller proportion are at risk of developing lesions.

Female rodents do not undergo a menstrual cycle with shedding of the endometrium akin to humans (with the exception of the spiny mouse [5]). Rather, an estrous cycle where the endometrium, in the absence of implantation, is reabsorbed by the activity of infiltrating leukocytes. As such, rodents will not spontaneously develop endometriotic lesions, and animal models to date have required manual implantation of endometrial fragments into the abdominal space. The vast majority of these models require surgery: either a ventral midline abdominal incision with uterine tissues sutured to visceral structures, such as the renowned rat autologous model [6, 7]; and/or a dorsal flank incision and ovariectomy, typically followed by estrogen supplementation [8, 9] (for reviews of rodent models used for endometriosis research see Pullen et al. (2011) [10] and Greaves et al. (2017) [11]).

It is widely acknowledged that long-lasting modulation of somatosensory processing can occur in animals following incisional surgery or similar techniques. This includes changes in the sensitivity of both peripherally and centrally located neurons [12, 13]; altered expression of proteins integral to neurotransmission, such as spinal metabotropic glutamate receptors [14]; as well as sensitization of the neuroimmune system, demonstrated by increased reactivity of spinal microglia and heightened somatosensensory activity [15]. Therefore, while many studies utilize sham controls, subtle changes in proteins or behaviors of interest in models of endometriosis may be masked by a relatively larger effect of the surgery. This limits the use of available models for experiments that are particularly sensitive to tissue injury, such as observations of the nervous system (as mentioned above), and therefore may particularly impact on studies of peripheral and central sensitization, and pain. These investigations remain imperative, as the severity of pain reported by women seldom correlates with the extent and duration of endometriosis [16], suggesting a more complex etiology beyond that observed at the peripheral lesion site.

Animal models of endometriosis that involve ovariectomy have the additional complication of being impracticable for studies of physiological functions that require natural fluctuations in sex hormones, such as fertility. It has long been hypothesized that endometriosis lesions thrive under the influence of heightened or prolonged estrogen stimulation [17, 18], since symptoms of the condition often first present at, or soon after menarche, and improve when estrogen levels fall at menopause; and the endometrium involutes in the absence of estrogen. Consequently, manipulation of sex hormones in basic scientific work has further implicated a role for estrogen in lesion development, where exogenous administration of estradiol in ovariectomized rodents enhances endometrial implant growth [19, 20]; is modulated by estrogen receptor signaling [21]; and can lead to recurrence of lesions that have previously regressed [22]. Researchers have also recently developed a hormonal protocol that transforms the rodent endometrium into a phenotype that mimics human menstrual debris, which is subsequently collected for use in an animal model [9]. Therefore, while there are many benefits of controlling sex hormones for endometriosis research, in many cases the continuous systemic estrogen stimulation is of supra-physiological levels and may not necessarily reflect the clinical setting.

In addition to altered sex hormone activity, the variable susceptibility among human females in developing endometriosis lesions is also thought to be influenced by genetic (and environmental/epigenetic) factors [23]. Comparing lesion characteristics in rodent models of diverse genetic backgrounds, where the susceptibility of each strain is unknown, may complicate research findings. Determining the behavior of specific rodent strains may therefore provide further insight into the varied types of endometriosis lesions and their associated symptoms. For example, C57BL/6 and BALB/c are two strains of commonly used wild-type mice that are known to differ in their immune profiles; the former considered Th1-dominant and the latter Th2-dominant in the immune response [24]. This affects the timing, composition, and location of cytokine release in response to specific immune insults, and hence how each strain might respond to donor tissue in endometriosis models.

Given endometriosis continues to be an area of significant unmet medical need, and the mechanistic disconnects between clinical presentation of the condition and animal models, we sought to refine and carefully characterize an animal model of endometriosis in mice. In this study, we have utilized a minimally invasive, gonad intact mouse model of endometriosis which may be compatible with experiments that are sensitive to surgery or incisional injury, and sex hormone manipulation. Further, we have considered the extent of lesion development in two genetically diverse mouse strains, during estrous stages of relatively high- and low-estrogen concentrations, and with increasing amounts of inoculated endometrial tissue.

Methods

Animals

Cytological evaluation of vaginal smears from 12 ± 3-week old, virgin female mice (weighing 20.6 ± 2.0 g) was used to determine current estrous stage, as described previously [25]. C57BL/6NHsd (C57BL/6; $n = 43$ donors and 43 recipients) or BALB/c ($n = 38$ donors and 43 recipients) mice in proestrus and estrus were selected for experimental use, corresponding to the respective estrous stages of relatively high and low estrogen [26]. Animals were obtained from the University of Adelaide Laboratory Animal Services; all experimental procedures were performed in accordance with the National

Health and Medical Research Council Australian code for the care and use of animals for scientific purposes (eighth edition, 2013) and the University of Adelaide Animal Ethics Guidelines, and were approved by the University of Adelaide Animal Ethics Committee.

Induction of endometriosis

Donor mice were anesthetized by isoflurane inhalation, sacrificed by cervical dislocation and their uterus removed. Tissues were placed immediately in cold (4°C) phosphate-buffered saline (0.01 M PBS composed of 13.7 mM NaCl, 0.27 mM KCl, 0.15 mM KH_2PO_4 and 0.8 mM Na_2HPO_4; pH 7.4) in a glass petri dish. Residual connective tissue, fat, the ovaries and cervix were removed, and each horn was opened along the mesometrial border. The uterine horns were then pinned flat to the Sylgard-coated base (Dow Corning; Michigan, USA) of the glass petri dish using entomology pins. The endometrium was removed by sharp dissection, measured for wet weight, and sectioned into 2–3 mm^2 fragments. Once the desired amount of endometrium was collected (7.5, 15, 25, or 40 mg), the fragments were suspended in a syringe with 0.5 ml sterile saline (0.9% NaCl; RT) and passed once through a 21-gauge needle. This was to ensure smooth delivery of content to recipient animals.

Recipient mice of syngeneic strain and identical estrous stage were then intraperitoneally injected with the donor endometrial fragment suspension (ENDO mice) at the ventral midline between the left inguinal nipples. Control recipient mice were injected with an equal volume of sterile saline only. Following 21 days development, ENDO mice were deeply anesthetized with isoflurane gas and decapitated, to remove blood and allow for an unobstructed view of the abdominopelvic cavity. After thorough examination, the number and location of endometriosis-like lesions was recorded. Identified lesions and control tissues for histological comparison from saline-injected mice (endometrium, lymph nodes, gastrointestinal tract, fat) were immediately fixed with cold (4°C) paraformaldehyde fixative (4% in 0.01 M PBS; pH 7.2) for 4–6 h.

Histological assessment

Endometriosis-like lesions and control tissues were further fixed in 10% neutral-buffered formalin (Chem-Supply; South Australia, Australia) overnight (4°C), placed in cassettes and submerged into 70% ethanol, then dehydrated in graded alcohols, cleared with xylene, and embedded with warmed liquid paraffin wax. Once solidified, serial sections of 5 μm were cut using a rotary microtome and collected onto albumin-coated slides. Routine hematoxylin and eosin staining was then performed, and the slides scanned using a NanoZoomer (Hamamatsu Photonics; Shizuoka Pref., Japan) and viewed with NanoZoomer Digital Pathology software view.2 (Histalim; Montpellier, France). Lesions were assessed in a blinded fashion for the presence of both glands and stroma, which are typically pre-requisite for a confirmed diagnosis of endometriosis in humans [27]. Parameters including inflammatory cell infiltration, blood vessels, connective tissue, and the presence of cysts were also recorded. Immunohistochemical staining for F4/80 was performed to further confirm the presence of macrophages within endometriosis-like lesions (for details see Supplementary Figure S1). Only lesions classified as dense or cystic type were counted toward the total number of lesions obtained from an ENDO animal (see description of lesion characteristics in Results). The size of endometriosis-like lesions was defined as the maximum diameter of the cut surface area in histological sections. Note that due to their variable shape, lesions were orientated during embedding so that the greatest dimension would be sectioned longitudinally.

Statistical analysis

In total, 14 experimental groups were analyzed: C57BL/6 and BALB/c mice in proestrus injected with 7.5, 15, 25, and 40 mg donor endometrial tissue (eight groups proestrus); and C57BL/6 and BALB/c mice in estrus injected with 15, 25, and 40 mg endometrium (six groups estrus).

SPSS Statistics 24 software (IBM; New York, USA) was used for statistical analyses and GraphPad Prism 7 software (GraphPad Software Inc.; California, USA) was used to generate summary graphs. A logistic regression model was used to investigate the association of at least one lesion present (lesion success) with the mouse model variables; a linear regression model and two-way ANOVA with Holm-Šídák multiple comparisons were performed to assess for associations between the total number of lesions, after determining that the assumptions of a linear model were upheld; a logistic generalized estimating equation model was performed to analyze the associations between lesion type (cystic or dense) as well as lesion locations; and a linear mixed-effects model was used to determine differences in lesion sizes.

The independent variables in these statistical models were mouse strain (C57BL/6 or BALB/c), estrous stage at induction (proestrus or estrous), and mass of injected tissue (7.5, 15, 25 or 40 mg), which were analyzed individually or with strain–stage, stage–mass, or mass–strain interactions. From the statistical models, an odds ratio or estimate, 95% confidence interval, comparison P value and interaction P value (where applicable) were calculated. A P value of <0.05 was considered statistically significant. Descriptive values of ENDO induction parameters and lesion characteristics are presented as mean ± standard deviation, whilst statistical data relating to lesion location, incidence, total number, and mouse strain are presented as mean ± standard error.

Results

Endometriosis-like lesions develop with distinct characteristics

Endometriosis-like lesions were successfully established in our minimally invasive mouse model. No interruptions to the estrous cycle were observed in recipient ENDO mice throughout the 21-day development period, indicating that the ovaries were intact and functioning as normal. The 7.5 mg recipient group were injected with an average of 7.6 ± 0.2 mg donor endometrium in 5.1 ± 0.3 pieces ($n = 12$); the 15 mg ENDO animals 16.3 ± 1.2 mg in 9.0 ± 1.5 pieces ($n = 26$); the 25 mg group with 25.0 ± 2.4 mg in 18.5 ± 4.0 pieces ($n = 24$); and 40 mg ENDO animals 41.1 ± 2.3 mg in 28.8 ± 3.5 pieces ($n = 24$). No overt effects were observed on the reproductive organs or tissues adjacent to endometriosis-like lesions in ENDO mice, except for occasional areas of erythema surrounding the lesions. Following histological processing and imaging, all endometriosis-like lesions collected from ENDO mice were initially classified into one of three categories based on their characteristics: dense, cystic, or necrotic-type lesions.

Macroscopically, dense-type lesions appeared opaque and light pink to deep red in color with a smooth surface, in some cases speckled with darker red blood vessels, and ranged from 221 to 4260 μm in length (average lesion length 1219 ± 832.8 μm; $n = 45$) (Figure 1A). On histological inspection, it was confirmed that dense lesions contained both epithelial (glandular) and stromal endometrial cells (Figure 1D). These lesions were encapsulated by a sheath of connective tissue, vascularized with single-layer walled small blood vessels, and commonly infiltrated by inflammatory cells,

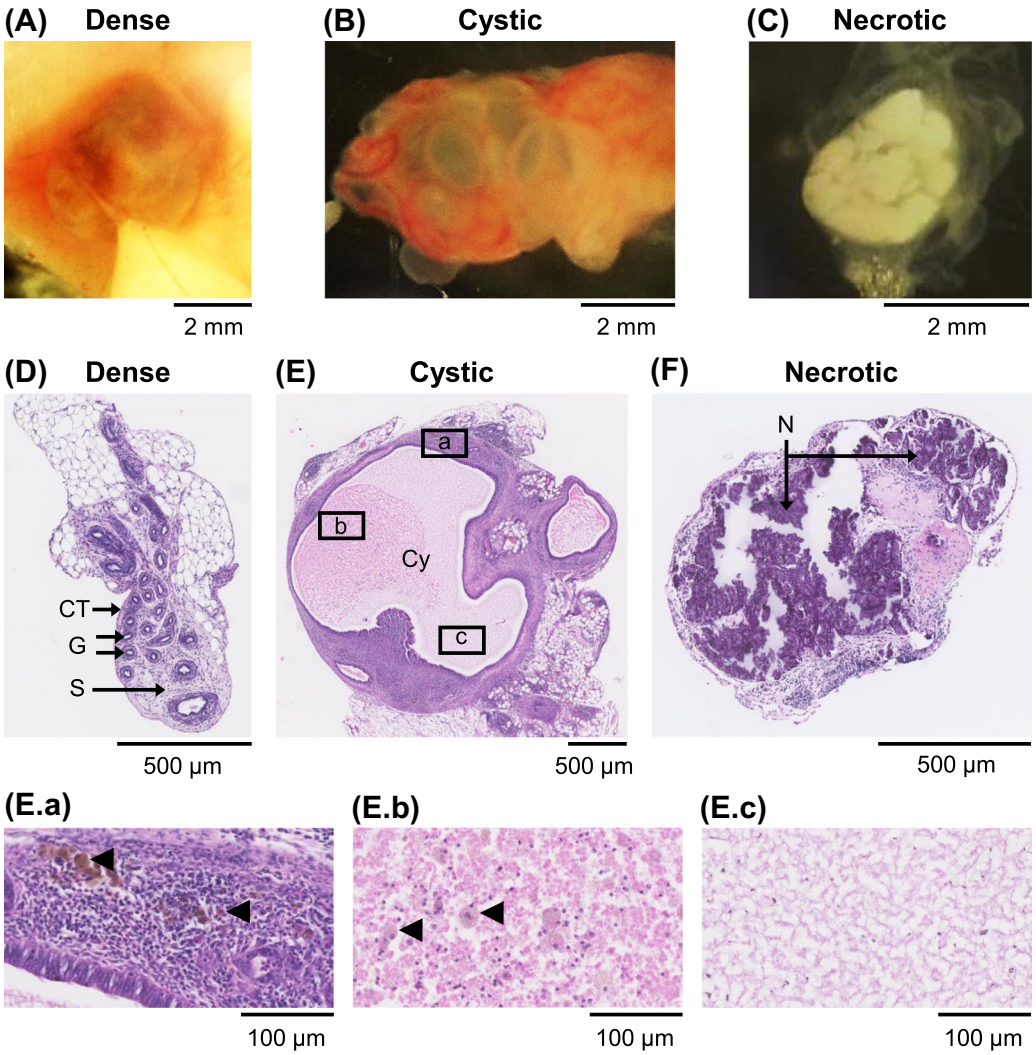

Figure 1. Macroscopic and histological characteristics of endometriosis-like lesions developed in the minimally invasive mouse model of endometriosis (ENDO). (A) Macroscopic image of a dense-type lesion embedded within gonadal white adipose tissue. The lesion is opaque and pink–red colored, and the surface is generally smooth; note connective tissue strand adhering the anterior surface of the lesion to an adjacent region of fat. (B) Cystic-type lesions had a "bubbled" appearance and were often translucent. (C) Necrotic-type lesions were easily identified by their striking white color and small size. (D) Histological example of a dense-type lesion, showing the connective tissue capsule (CT), endometrial glands (G), and endometrial stroma (S). (E) Cystic-type lesions contained one or more fluid-filled cysts (Cy). Within the stroma (E.a, inset) and cysts (E.b, inset), macrophages (arrowheads) often stained brown within their cytoplasm, indicating possible hemosiderin deposition. (E.c, inset) Cysts also contained a lightly eosinophilic web-like structure with sporadic nuclei of an unidentified cell type. (F) Necrotic-type lesions showed areas of hematoxylin-rich tissue necrosis (N), with minimal discernible endometrial glands or stroma. Magnification in (E.a-c) 40× inset.

such as macrophages and lymphocytes (identified by their morphological characteristics). Identified macrophages often contained areas of punctate brown staining akin to hemosiderin deposition, as has been observed in other animal models [28] and human endometriosis lesions [29].

Cystic-type lesions were characterized by the presence of a fluid-filled cyst in addition to endometrial glands and stroma. Cystic lesions were again light pink in color, although translucent due to the cysts; in many cases, the donor endometrial fragments could be seen inside. The cysts often had a "bubbled" or multilobed appearance (Figure 1B and E). These lesions were commonly surrounded by a capsule of connective tissue that appeared contiguous with adjacent structures. Cystic-type lesions were also vascularized, and displayed inflammatory cell infiltrate within the stroma (Figure 1E-a). Cysts typically contained inflammatory cells (including macrophages and lymphocytes) and red blood cells (Figure 1E-b), as well as a yet-unidentified lightly eosinophilic web-like structure (Figure 1E-c). The presence of macrophages in lesions was further confirmed by distinct F4/80-positive structures within the cyst lumen and stroma (Supplementary Figure S1). Cystic-type lesions were generally larger than dense lesions, ranging from 503 to 3700 μm (average 1990 $\pm$ 847.1 μm; $n = 50$).

Necrotic lesions were ubiquitously white in color with an irregular surface, and small in size (range 564 to 650 μm; average 606.5 $\pm$ 35.87 μm; $n = 4$) (Figure 1C). Histologically, they were defined by a majority presence of necrosis within a lesion, determined as areas of dense hematoxylin staining without discernible cellular or tissue structure (Figure 1F). This meant that in many necrotic lesions obvious glands and stroma were not identified. Interestingly, necrotic lesions were only observed in ENDO animals induced with proestrus endometrial tissue. Due to the single time-point of tissue collection in this study, it is unknown whether necrotic lesions

were previously fully formed lesions that were degenerating at the time of collection, or if they never formed lesions and were deteriorating donor endometrial tissue left over from the initial ENDO injection. For these reasons, and that glands and stroma were not consistently present, necrotic-type lesions were excluded from further analysis.

Endometriosis-like lesions develop in diverse peritoneal locations

The location of endometriosis-like lesion development was random across the various ENDO groups; there were no significant associations with estrous stage, mass of injected tissue, or strain of mouse. Lesions formed in several locations within the peritoneal cavity, typically on the anterior surfaces, likely because of the posture and gravity in quadrupedal animals. Most often lesions tended to form on connective tissue-like structures, such as mesenteric attachments between the stomach and pancreas (47/95 lesions; 49.5% total). It was common to also observe lesions on the anterior abdominal wall, at a level typical of the injection site (18/95 lesions; 18.9% total), as well as within fatty structures such as the gonadal white adipose tissue (24/95 lesions; 25.3% total) (Figure 2). Few lesions (3/95 lesions; 3.1% total) formed in the subcutaneous space, likely due to residual fragments of endometrial tissue embedding at the insertion point upon needle withdrawal. A single lesion also formed on connective tissue anchoring the descending colon to the posterior abdominal wall (1.1% total), and two lesions were found on connective tissue bridging the posterior uterine body with the anterior descending colon/rectum (2.1% total).

Successful development of endometriosis-like lesions is dependent on the quantity of donor endometrium and estrous stage

Controlling for both mouse strain and stage, the incidence of endometriosis-like lesion development increased as the amount of donor endometrial tissue injected into ENDO mice progressed from 7.5 to 40 mg. Collectively amongst the ENDO groups, the rate of lesion establishment was 33.3% for animals injected with 7.5 mg ($n = 4/12$); 69.2% for 15 mg animals ($n = 18/26$); 83.3% for those in the 25 mg group (20/24); and 100% for recipient mice injected with 40 mg endometrium ($n = 24/24$). Using the 7.5 mg group as reference (14% estimated probability of developing lesions), 15 mg ENDO animals were 16.9 times more likely to develop lesions (73% probability; $P = 0.004$), 48.5 times more likely with 25 mg (88% probability; $P = 0.001$), and were all expected to develop lesions in the 40 mg group (100% probability; $P < 0.001$).

Interestingly, endometriosis-like lesions were 1.9 times more likely to establish in proestrus as opposed to estrus ($P = 0.009$), when controlled for both strain and group mass. For C57BL/6 ENDO mice, lesions were observed in 33.3% ($n = 2/6$) of animals injected with 7.5 mg tissue in proestrus, and in all animals with 15 mg and above (100%; 19/19). BALB/c mice in proestrus developed lesions in 33.3% of 7.5 mg animals ($n = 2/6$), 71.4% of 15 mg animals ($n = 4/7$), and 100% of animals injected with 25 and 40 mg of donor endometrial tissue ($n = 12/12$) (Figure 3A). In contrast, lesions developed in only half of 15 mg C57BL/6 and BALB/c ENDO mice in estrus (50%; $n = 3/6$ per strain), two-thirds of 25 mg mice (66.7%; $n = 4/6$ per strain), and all animals at 40 mg (100%; $n = 6/6$ per

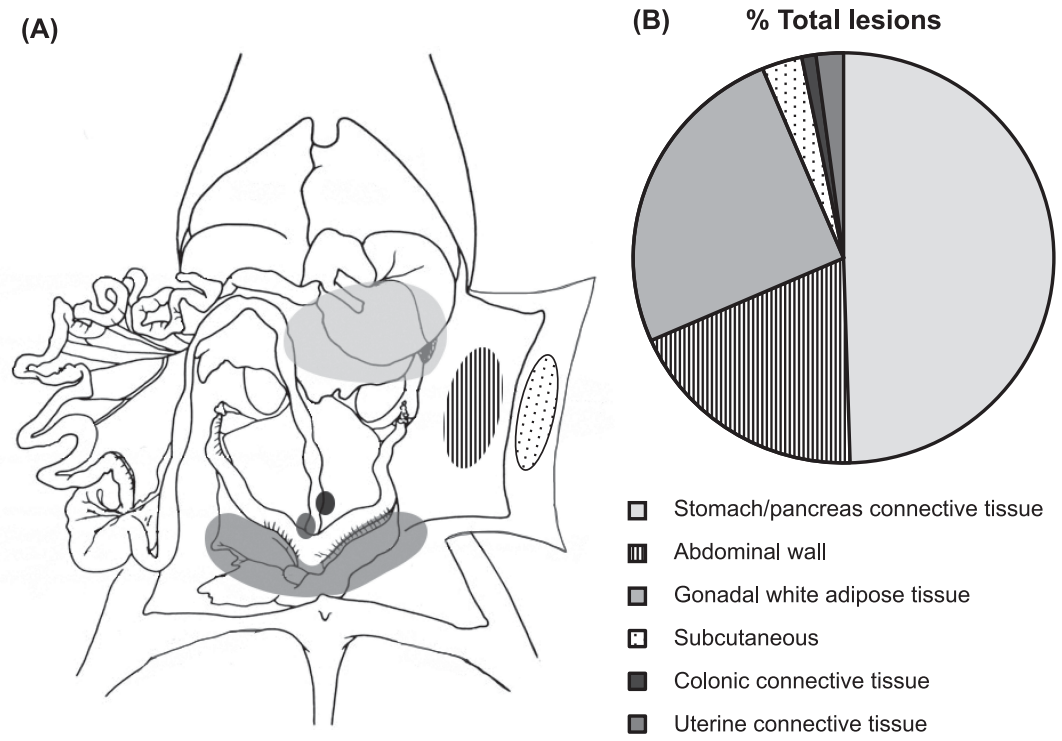

Figure 2. Anatomical locations of endometriosis-like lesions established in ENDO mice. (A) Schematic diagram of the anterior view of the internal female mouse anatomy, depicting the locations of endometriosis-like lesions established in ENDO mice. Commonly, lesions were found most superiorly on connective tissue attachments near the stomach and pancreas, on the anterior abdominal wall (ipsilateral to the injection site), and inferiorly within the gonadal white adipose tissue. Few lesions formed in the subcutaneous space (also ipsilateral to injection), on connective tissue of the colon, and connective tissue between the colon and uterus. (B) Summarized data of the proportion of lesions in each location. Outline of mouse anatomy in (A) adapted with permission from Elsevier and Jackson Laboratories [60].

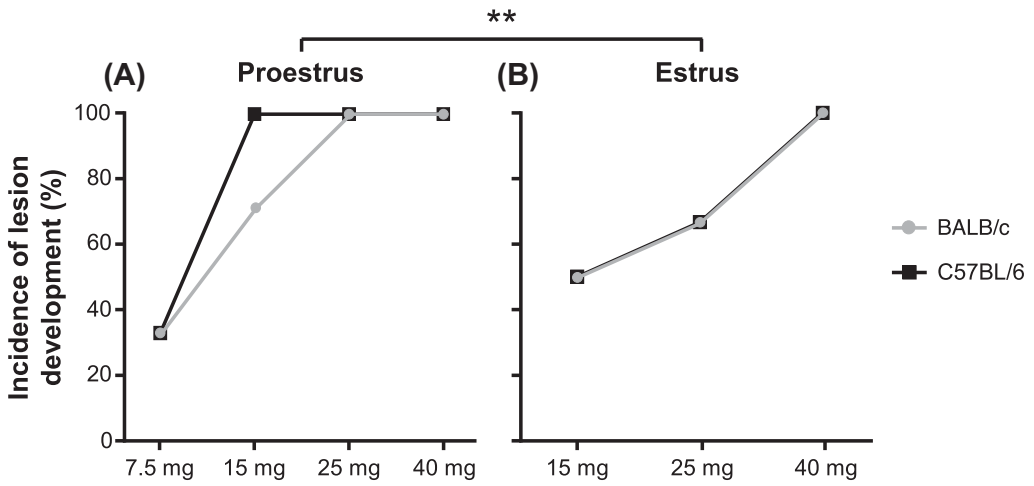

Figure 3. Modulation of endometriosis-like lesion prevalence in ENDO mice by the quantity of donor endometrium and estrous stage at induction. (A) Proportion of C57BL/6 and BALB/c ENDO animals in proestrus, grouped by mass of donor endometrial tissue, which developed at least one endometriosis-like lesion 3 weeks post-injection. (B) Proportion of animals that successfully established lesions when induced in estrus. Overall, the probability of lesion development increased as the mass of donor endometrial tissue increased (statistics not shown), and was also greater in proestrus (high estrogen) than estrus (low estrogen). However, there was no effect of mouse strain on lesion establishment. '**' denotes $P < 0.01$.

strain) (Figure 3B). ENDO animals in estrus with 7.5 mg donor tissue were not analyzed in this study.

No mouse strain effect was observed for the successful development of lesions. The incidence of lesion development was equal in both C57BL/6 and BALB/c mice, except at 15 mg in proestrus where C57BL/6 ENDO mice had a slightly increased rate (by 28.6%) compared to BALB/cs (100% vs 71.4% respectively; 95% CI: –0.05, 0.62).

Number of endometriosis-like lesions is modulated by the quantity of donor endometrium, estrous stage and mouse strain

In addition to the frequency of ENDO animals developing lesions, there was a positive correlation between the number of total endometriosis-like lesions per animal and the mass of donor endometrium. Controlled for strain and stage, animals injected with 7.5 mg tissue developed 0–1 lesions (mean 0.13 ± 0.21); 15 mg animals 0–2 lesions (mean 0.79 ± 0.13); 25 mg-injected animals 0–3 lesions (mean 1.25 ± 0.14); and 40 mg animals 1–3 lesions (mean 1.67 ± 0.14) (all pairwise comparisons $P \leq 0.033$).

In C57BL/6 ENDO mice, a greater total number of lesions per animal were observed in the proestrus groups as opposed to estrus groups. On average 7.5 mg proestrus mice developed 0.33 ± 0.24 lesions; 15 mg mice developed 1.14 ± 0.22 lesions in proestrus versus 0.50 ± 0.24 lesions in estrus; the 25 mg proestrus group developed 1.67 ± 0.24 lesions versus 0.67 ± 0.24 lesions in estrus; and the 40 mg groups developed 1.67 ± 0.24 versus 1.50 ± 0.24 lesions, respectively. Therefore overall, proestrus C57BL/6 mice had a probability of developing 0.60 ± 0.21 more lesions at any given group mass compared to those in estrus ($P = 0.005$), with the most significant difference at 25 mg (probability of 1.00 ± 0.34 more lesions in proestrus than estrus; $P = 0.004$) (Figure 4A). This is reiterated by a reduced average mass of endometrium that was required to obtain 0 (7.68 ± 0.11 vs 19.66 ± 2.07 mg; $P = 0.004$), 2 (22.03 ± 3.25 vs 37.97 ± 0.62 mg; $P = 0.017$) and 3 lesions (34.77 ± 5.84 vs >40 mg) in proestrus versus estrus, respectively (Figure 4B). The pattern for the predicted number of lesions per group mass in proestrus was an increase by 0.81 ± 0.33 lesions from 7.5 mg to 15 mg ($P = 0.014$), which then remained stable at 25 mg (+0.52 ± 0.33 lesions from 15 mg to 25 mg; $P = 0.113$) and 40 mg (+0.00 ± 0.34 lesions from 25 mg to 40 mg; $P = 1.000$). In estrus, the 15 mg and 25 mg groups developed similar numbers of lesions (+0.17 ± 0.34 lesions from 15 mg to 25 mg; $P = 0.627$) until 40 mg, which showed an increase by 0.83 ± 0.34 lesions (from 25 mg; $P = 0.015$).

In contrast, BALB/c ENDO mice developed similar total numbers of lesions per group mass regardless of estrous stage (Figure 4C). For 7.5 mg animals in proestrus, the average number of lesions was 0.33 ± 0.29; 15 mg mice developed 1.00 ± 0.26 lesions in proestrus versus 0.86 ± 0.28 lesions in estrus; the 25 mg proestrus group developed 1.50 ± 0.26 lesions versus 1.60 ± 0.23 lesions in estrus; and the 40 mg groups developed 2.33 ± 0.21 versus 1.89 ± 0.24 lesions, respectively. Again, the absence of separation between proestrus and estrus is shown by similar average quantities of endometrium used to produce 1, 2, and 3 lesions (0 lesions 9.24 ± 2.32 vs 19.72 ± 2.27 mg, respectively; $P = 0.032$) (Figure 4D). The predicted number of lesions per group mass in proestrus did not significantly differ when compared incrementally until 40 mg, with an estimated 0.83 ± 0.33 more lesions than at 25 mg ($P = 0.013$). Although no differences were observed from 7.5 to 15 mg and then 15 to 25 mg, overall the 25 mg group was likely to develop 1.17 ± 0.39 lesions more than at 7.5 mg ($P = 0.003$) indicating a steady increase in lesion number throughout this range. In estrus, the predicted number of lesions increased from 15 to 25 mg (increase by 0.74 ± 0.36; $P = 0.039$) that remained stable from 25 to 40 mg (increase by 0.29 ± 0.34; $P = 0.390$). Between the 15 and 40 mg groups, lesions were estimated to increase by 1.03 ± 0.37 ($P = 0.005$).

Endometriosis-like lesion characteristics differ between mouse strains

A total of 95 lesions were collected from ENDO animals, 50 of which were cystic (52.6%) and 45 classified as dense type (47.4%). No differences in the ratio of cystic-to-dense lesions were detected in proestrus versus estrus ($P = 0.186$), where there were 33 (56.9%) cystic and 25 (43.1%) dense lesions in proestrus, versus 17 (45.9%)

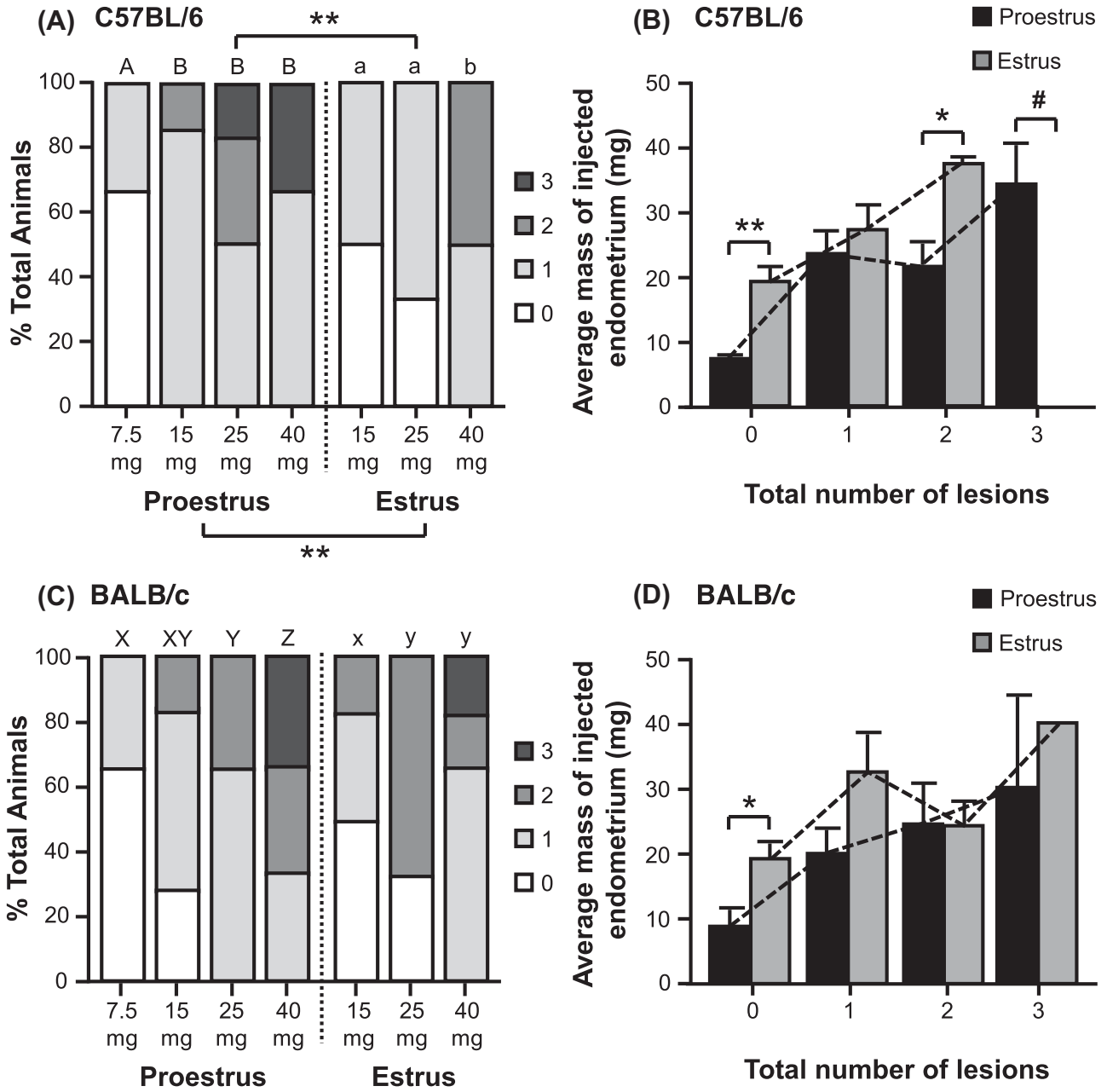

Figure 4. Total number of endometriosis-like lesions developed by ENDO mice is influenced by mouse strain, estrous stage, and mass of injected donor endometrial tissue. (A) Summarized data showing the proportions of total endometriosis-like lesions (0–3) developed by C57BL/6 mice in proestrus and estrus, at each mass of injected endometrial tissue. With increasing amounts of donor endometrium, more lesions established and, interestingly, a greater total number of lesions developed in proestrus compared to estrus (particularly at 25 mg). (B) This is supported by data displaying the average amount of endometrial tissue required to produce a given number of lesions. Here, the histogram indicates that to generate 0, 2, or 3 lesions proestrus C57BL/6 mice required less donor endometrial tissue compared to those in estrus. (C) While the total number of lesions was also greater with increased tissue mass in BALB/c mice, there was no statistical difference between the estrous stages. (D) A comparison between tissue volume and lesion number further indicates little effect of estrous stage influencing lesion number in BALB/c mice (except for 0 lesions). As indicated by the dashed lines linking the average mass of tissue per lesion number, note the similar patterns of lesion development between proestrus C57BL/6 mice in (B) and estrus BALB/c mice in (D), and vice versa. Bars not sharing the same superscript within the same panel are statistically different ($P < 0.05$). Uppercase letters are used for analysis within proestrus only, and lowercase letters are used for analysis within estrus. '$*$' denotes $P < 0.05$; '$**$' denotes $P < 0.01$; '#' denotes no lesions developed for statistical comparison.

cystic and 20 (54.1%) dense lesions in estrus (Figure 5A). Similar proportions of the lesion types were also observed across the group masses (all pairwise comparisons $P \geq 0.172$). ENDO mice with 7.5 mg donor tissue developed a total of two cystic and two dense lesions (50% each); 15 mg animals had 12 (57.1%) cystic and 9 (42.9%) dense lesions; 25 mg animals developed 13 (43.3%) cystic and 17 (56.7%) dense lesions; and finally 40 mg ENDO animals developed 23 (57.5%) cystic and 17 (42.5%) dense lesions (Figure 5B). However, BALB/c mice were 2.7 times more likely to develop cystic versus dense lesions compared to C57BL/6 mice ($P = 0.022$). From

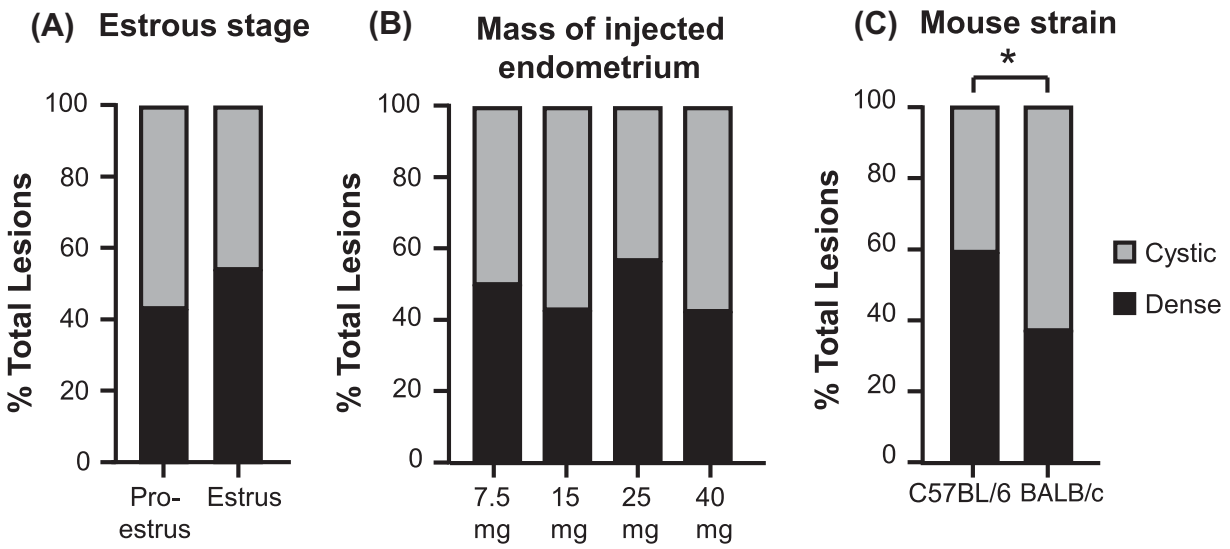

Figure 5. Probability of lesion type is altered in C57BL/6 and BALB/c ENDO mice. (A) Proportion of lesions characterized as cystic or dense type were similar in proestrus ($n = 58$ lesions from 40 animals) and estrus ($n = 37$ lesions from 26 animals). (B) Lesion type did not differ amongst different group masses (7.5 mg $n = 4$ lesions from 4 animals; 15 mg $n = 19$ lesions from 18 animals; 25 mg $n = 30$ lesions from 20 animals; and 40 mg $n = 40$ lesions from 24 animals). (C) There was a significant difference in the ratio of cystic-to-dense lesions between the C57BL/6 ($n = 46$ lesions from 34 animals) and BALB/c mouse strains ($n = 49$ lesions from 32 animals). BALB/c ENDO mice were 2.7 times more likely to develop cystic-type lesions than C57BL/6s. '$*$' denotes $P < 0.05$.

BALB/c mice, a total of 31 (63.3%) cystic and 18 (36.7%) dense lesions were collected, whereas C57BL/6 mice developed 19 (41.3%) cystic and 27 (58.7%) dense lesions (Figure 5C).

Adjusted for mass and strain, the average diameter of endometriosis-like lesions in proestrus was 1.42 ± 0.14 mm and in estrus 1.32 ± 0.18 mm ($P = 0.573$) (Figure 6A). Lesions from animals receiving 7.5 mg donor endometrium were 0.86 ± 0.44 mm in size; 15 mg animals had lesions 1.43 ± 0.19 mm in size; 25 mg animals had lesions 1.33 ± 0.16 mm in size; and 40 mg animals had lesions 1.86 ± 0.14 mm in size. Statistically, lesions from the 40 mg group were 1.00 ± 0.46 mm larger than those from 7.5 mg animals ($P = 0.033$) and 0.53 ± 0.21 mm larger than 25 mg animals ($P = 0.013$) (Figure 6B). Moreover, C57BL/6 mice developed lesions 1.22 ± 0.16 mm in size and BALB/c mice 1.52 ± 0.60 mm ($P = 0.104$) when controlled for mass and stage (Figure 6C). Post-hoc analysis interestingly revealed that within the 40 mg group there was a significant difference in lesion size between the mouse strains, where those from BALB/c ENDO mice were estimated to be 0.72 ± 0.27 mm larger than in C57BL/6 animals ($P = 0.010$) (Figure 6D). This difference is most likely due to the greater numbers of cystic-type lesions that were developed by BALB/c over C57BL/6 ENDO mice, and that cystic lesions were typically larger than dense lesions.

Discussion

In this study, we have carefully characterized the expression of endometriosis-like lesions in a minimally invasive, hormonally intact mouse model. Akin to the human condition, lesions were phenotypically heterogeneous; the vast majority presenting with well-organized endometrial glands and stroma, with or without cysts. Lesions were also of variable size, and adhered to a number of visceral structures within the peritoneum. We have demonstrated that viable lesions were able to form without using surgical procedures, or any exogenous sex hormone administration to either donor or recipient animals. In addition, our data show distinct patterns in lesion development dependent on the estrogen status, mouse strain, and mass of endometrial tissue injected.

Location of endometriosis-like lesion development is indiscriminate

The anatomical locations of lesions within the abdominopelvic cavity of ENDO mice did not form any discernible pattern, using the model permutations investigated in this study. Most lesions adhered on superficial peritoneal locations anywhere from the diaphragm to pelvis, most likely as a result of posture and gravity in quadrupedal mice. This is in contrast to humans, where the majority of lesions are typically distributed deeper within the pelvis due to the influence of a bipedal gait [30].

Regardless, the visceral tissues which lesions adhered to appeared similar to those observed in humans, with the exception that lesions did not form on the surfaces of the visceral organs. Most commonly, lesions established on the peritoneum and connective tissues around the stomach, with occasional lesions associated with the colon and uterus. These structures may resemble connective tissues within the female pelvis where endometriosis is frequent, including the uterosacral ligaments and the rectouterine pouch [31, 32]. The affected locations in our ENDO mice have also been described in models by other laboratories [9, 21]. Thus, both the phenotypic characteristics and anatomical distribution of lesions in our minimally invasive mouse model of endometriosis appear to be valid for its use in future investigations.

Prevalence and total number of endometriosis lesions increases with greater endometrial debris

As mentioned, the mechanical event believed to underpin the development of endometriosis is a retrograde menstruation, with the subsequent deposition, attachment and growth of endometrial fragments within the abdominopelvic cavity. In order to replicate this process in rodent models, including the method used in this

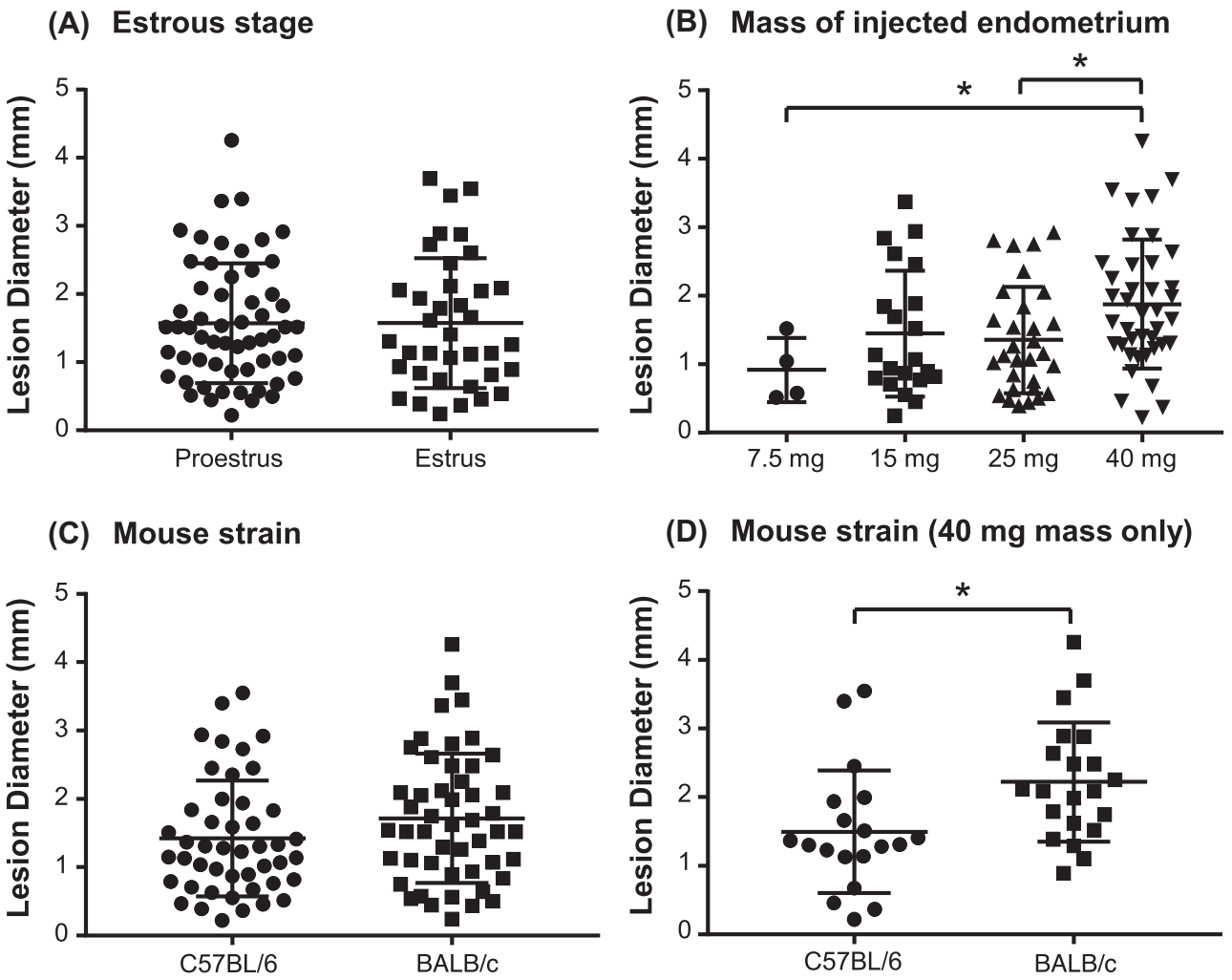

Figure 6. Maximal diameter of endometriosis-like lesions varied with mass of injected tissue and mouse strain. (A) The average size of lesions was similar regardless of estrous stage at the time of endometriosis induction. (B) However, lesions tended to be larger in animals injected with 40 mg donor endometrial tissue compared to the 7.5 and 25 mg groups. (C) While overall there was no difference in the size of lesions between the two mouse strains, at 40 mg only (D) lesion diameter was greater in BALB/c ENDO mice compared to C57BL/6s. '$*$' denotes $P < 0.05$.

study, endometrial fragments are administered by intraperitoneal injection. We observed that endometriosis-like lesions were more likely to develop in our ENDO animals as the amount of injected donor endometrium increased. In addition to the success rate, the total number of lesions also increased with greater doses of tissue.

This indicates that in our model we can reasonably predict the success and number of lesions that will develop depending on the amount of donor tissue injected (i.e. dose dependency). These results correlate with clinical observations, where it is consistently reported that, proportionally, endometriosis patients have earlier age of menarche, shorter menstrual cycle lengths, heavier menstrual effluent, and increased duration of menstrual flow than control counterparts [33, 34]; all characteristics that may contribute to large and frequent volumes of retrograde menstruation. Under normal conditions, refluxed endometrial debris is primarily cleared from the peritoneum by cells of the immune system. However, greater volumes of menstrual debris are hypothesized to overwhelm the peritoneal macrophage clearing mechanism, resulting in a permissive environment for developing endometriosis. Hence, one of the current successful therapies for preventing the recurrence of endometriosis is to suppress endometrial growth and menstruation (usually by hormonal manipulation, such as levonorgestrel [35]), thereby reducing the volume of menstrual debris for retrograde transport into the abdominopelvic cavity.

We also found that lesions developed from the greatest endometrial mass administered (40 mg) tended to be larger in size compared to those from smaller injections (7.5 and 25 mg). It may be speculated that administration of larger quantities of endometrial fragments challenges the immune clearance system to such an extent that the response mounted is insufficient and thus the lesions that establish consequently grow larger in size. In any case, the dose-response nature of our model may be vital for future studies investigating the effects of interventions on total lesion number, and supports that the quantity of injected endometrial tissue must be considered when comparing results between laboratories. Additionally, this flexible dosing approach allows for exploration of the signaling factors derived from the endometrial tissue that may condition the environment for endometriosis-like lesion development.

Endometriosis lesions are more likely to develop under conditions of naturally high estrogen

The endometrium is one of the primary targets for sex hormone stimulation, with estrogen producing many biological effects including hyperplasia, hypertrophy, and vascularization, and therefore favorable for the development of endometriosis lesions. While not wholly necessary for lesion establishment [21], administration of exogenous estrogen has been demonstrated in numerous studies to augment the total number, size, adherence, and invasiveness of lesions and promote tissue integrity [19, 21, 36].

Here, we are the first to investigate the effect of natural fluctuations in estrogen in freely cycling mice on the development of endometriosis, by inducing the condition during estrous stages of proestrus (preovulation; higher estrogen) and estrus (postovulation; lower estrogen). Other laboratories using naturally cycling rodents typically use estrus [37] or diestrus endometrium [38, 39] (the latter hormonally comparable to menses in humans) and/or administer exogenous estrogen at least to the donor animal regardless of estrous stage [40]. Endometriosis-like lesions in this study were achieved at a significantly higher rate during proestrus than in estrus, irrespective of mouse strain or volume of donor tissue. C57BL/6 mice also developed a greater total number of lesions in proestrus, although no other differences in lesion characteristics such as size, type, or location were found to be dependent on estrous stage.

Thus, our data show that several previous experimental observations of endometriosis can be replicated in rodent models without the use of additional hormones. In addition, we further support a role for estrogen in enhancing susceptibility to lesion formation. That we did not observe other estrous-dependent variations in lesion characteristics likely relates to a limitation of our minimally invasive mouse model, which is that the inoculated donor endometrium was healthy. In addition, the tissue was not menstrual-like [9] nor at an equivalent estrous stage to the menstrual phase in humans [38], as our aim was to characterize lesion development using endometrium influenced by natural periods of low and high estrogen. While we were able to positively identify endometriosis-like lesions generated from such tissue, considerable evidence from studies on human lesions and eutopic menstrual tissue from endometriosis patients has shown to be atypical compared to healthy endometrium.

One of the major purported differences is that the endometrium from women with endometriosis may be functionally resistant to progesterone stimulation [41]. The failure of progesterone to act appropriately ultimately affects the phenotype of endometrial tissue shed at menstruation, which displays a prolonged reduction in anti-inflammatory signaling, and highly robust, pro-growth endometrial debris under mostly estrogenic stimulation [42]. Therefore, while the donor tissue used in our model may not fully mimic the endometrial characteristics observed in endometriosis patients, it does not preclude from using donor tissues in future studies that more accurately represent the pathophysiology of lesion development in humans.

Quantity and characteristics of endometriosis lesions differ between mouse strains of diverse genetic backgrounds

Another novelty of the present study is that we comprehensively compared and contrasted the development of endometriosis-like lesions in two genetically diverse, wild-type inbred mouse strains. Using a surgical model with estrogen supplementation, only one study to our knowledge has investigated lesion formation in similar mice, which reported no strain differences in their number or histological characteristics in recipients with a maximum 15 mg donor tissue [43]. These experimental conditions would most closely resemble our 15 mg proestrus group. Considering this permutation alone, we would also be unable to discern any variations in lesion number or characteristics between the mouse strains. However, when analyzed in combination with greater volumes of endometrium and at different estrous stages, several critical differences were established.

C57BL/6 mice generated a significantly greater total number of lesions in proestrus than estrus; an effect that was not observed in BALB/cs. Based on the previous information linking sex hormones and endometriosis, the higher lesion count in proestrus C57BL/6 mice likely also reflects the effects of relatively high estrogen levels at induction (and therefore a pro-survival, pro-growth, pro-vascularization microenvironment surrounding the endometrial debris). It was unexpected and unknown at this stage why BALB/c mice did not show a similar cycle sensitivity.

As speculated, mouse strain differences in the development of endometriosis lesions could be attributed to variations in their immune responses to the donor endometrial tissue. In addition to an excess of refluxed menstrual debris, dysregulation of peritoneal macrophage function has also been implicated in the implantation and growth of endometrial lesions [44]. The specific mechanisms contributing to the evasion of ectopic endometrium from immune clearance are vast, and include decreased cell cytotoxic activity [45]; altered levels of pro-inflammatory cytokines, growth and angiogenic factors [46]; decreased recognition of ectopic endometrium [47]; and increased immune cell apoptosis [48] (for reviews see Christodoulakos et al. (2007) [49]; Herington et al. (2012) [44]).

Although immune responses of the wild-type mice used in this study may not necessarily have been inappropriate, their different genetic regulation may result in activation of distinct inflammatory cells, signaling cascades, and mediators that ultimately determines the fate of the endometrial debris. Previous studies have demonstrated that C57BL/6 and BALB/c mice exhibit strikingly different cytokine signatures to several bacterial infections [50, 51]; show estrous cycle-dependent [52] and brain region-specific [53] inflammatory responses to an identical stimulus; and are diversely susceptible to experimental autoimmune conditions [54], and tumorigenesis [55, 56].

In general, C57BL/6 mice are genetically inclined to mount a Th1/M1 macrophage-dominant immune response, characterized by an IFNγ-mediated upregulation of multiple pro-inflammatory mediators such as TNFα, IL-1β, IL-6, and iNOS. BALB/c mice alternatively produce Th2/M2 macrophage-dominant responses, an IL-4-driven milieu of anti-inflammatory cytokines, including IL-5, IL-8, and IL-10 [57, 58]. A previous study showed that adoptive transfer of M1 macrophages into the peritoneum of recipient mice resulted in significantly reduced growth of endometriosis-like lesions, while conversely enhanced growth in the presence of M2 macrophages [59]. A similar phenomenon could therefore be associated with the opposing predominant lesion types observed here, where C57BL/6 mice (Th1/M1) developed more lesions with small dense-type characteristics, as opposed to the large cystic-type in BALB/cs (Th2/M2).

Our findings highlight that caution should be taken when translating results between different strains of mice (and between species), and to carefully consider strain prior to the initiation of new experiments. Given that macrophages from peritoneal fluid and ectopic lesions in endometriosis patients express higher levels of M2 markers [59], we suggest that BALB/c mice may be a preferred mouse strain that more closely represents the human condition (and therefore better suited for human xenograft mouse models), although

further investigations are necessary. Future studies conducting screening of novel pharmacological interventions should consider conducting tests in multiple strains to avoid unfortunate false-negative results. Additionally, these data point to the need for personalized medicine in the treatment of endometriosis through phenotyping of the lesion types and targeted treatment selection.

Conclusions

As with all rodent models of endometriosis, the absence of natural menstruation means that care must be taken when translating research to humans. Nevertheless, it is hoped that the minor interventions required to successfully develop lesions in this study may be particularly beneficial for researchers investigating endometriosis-induced alterations to the CNS, reproductive processes or any other biological system that is sensitive to surgery or the manipulation of sex hormones. Examples of potential applications include maternal or early life influences of lesion development, the impact of surgical removal of lesions, contributions to and consequences of pain and central sensitization, and the effect of lesions on fertility. With such possibilities, this model may be useful for studying new molecular targets and therapeutics, to ultimately provide better treatment outcomes for women often long-suffering with endometriosis.

Supplementary data

Supplementary data are available at *BIOLRE* online.

Supplementary Figure S1. Immunohistochemical labeling for the macrophage-specific marker F4/80 in endometriosis-like lesions from ENDO mice. (A) Low-magnification example of a cystic-type lesion from an ENDO mouse displaying macrophage infiltration within the cyst lumen and throughout the stroma ($n = 6$). In brief, sections of endometriosis-like lesions were blocked for nonspecific staining of tissues, then incubated in 1.25 μg/ml rat anti-mouse F4/80 primary antibody (#14-4801-82; clone BM8; eBiosciences; San Diego, CA), overnight at 4°C. After washing, 1 μg/ml biotinylated rabbit anti-rat secondary IgG (#BA-4001; Vector Laboratories; Burlingame, CA) was applied to sections (40 min; RT), followed by Vectastain ABC-HRP reagent (#PK-4000; Vector Laboratories; Burlingame, CA) (30 min; RT). The immunocomplex was visualized with precipitation of DAB (#K3468; Dako; Carpinteria, CA) (15 min; RT) and lightly counterstained with hematoxylin. Negative controls were performed by omitting the primary or secondary antibody. (B, inset) Higher magnification of F4/80-positive macrophages within the cyst of the endometriosis-like lesion (arrows). (C, inset) F4/80-positive macrophages were also clearly visible at higher magnification within the surrounding stroma of endometriosis-like lesions (arrows). Scale bar in (C) also applies to (B). Magnification in (B, C) 40× inset.

Acknowledgments

We thank Mrs Kathryn Batra, Mrs Emily Schneider, and Ms Kavita Panir for assistance with histological processing of tissues. We also thank Ms Suzanne Edwards, Dr Jonathan Tuke, and Ms Jiajun Liu for guidance with statistical analyses.

References

1. Eskenazi B, Warner ML. Epidemiology of endometriosis. *Am J Pathol* 1997; **24**:547–556.
2. Sampson JA. Peritoneal endometriosis due to the menstrual dissemination of endometrial tissue into the peritoneal cavity. *Am J Obstet Gynecol* 1927; **14**:422–469.
3. Halme J, Hammond MG, Hulka JF, Raj SG, Talbert LM. Retrograde menstruation in healthy women and in patients with endometriosis. *Obstet Gynecol* 1984; **64**:151–154.
4. O DF, Roskams T, Van den Eynde K, Vanhie A, Peterse DP, Meuleman C, Tomassetti C, Peeraer K, D'Hooghe TM, Fassbender A. The presence of endometrial cells in peritoneal fluid of women with and without endometriosis. *Reprod Sci* 2017; **24**:242–251.
5. Bellofiore N, Ellery SJ, Mamrot J, Walker DW, Temple-Smith P, Dickinson H. First evidence of a menstruating rodent: the spiny mouse (Acomys cahirinus). *Am J Obstet Gynecol* 2017; **216**:40.e41–40.e11.
6. Vernon MW, Wilson EA. Studies on the surgical induction of endometriosis in the rat. *Fertil Steril* 1985; **44**:684–694.
7. Berkley KJ, Cason A, Jacobs H, Bradshaw H, Wood E. Vaginal hyperalgesia in a rat model of endometriosis. *Neurosci Lett* 2001; **306**:185–188.
8. Hull ML, Escareno CR, Godsland JM, Doig JR, Johnson CM, Phillips SC, Smith SK, Tavaré S, Print CG, Charnock-Jones DS. Endometrial-peritoneal interactions during endometriotic lesion establishment. *Am J Pathol* 2008; **173**:700–715.
9. Greaves E, Cousins FL, Murray A, Esnal-Zufiaurre A, Fassbender A, Horne AW, Saunders PT. A novel mouse model of endometriosis mimics human phenotype and reveals insights into the inflammatory contribution of shed endometrium. *Am J Pathol* 2014; **184**:1930–1939.
10. Pullen N, Birch CL, Douglas GJ, Hussain Q, Pruimboom-Brees I, Walley RJ. The translational challenge in the development of new and effective therapies for endometriosis: a review of confidence from published preclinical efficacy studies. *Hum Reprod Update* 2011; **17**:791–802.
11. Greaves E, Critchley HO, Horne AW, Saunders PT. Relevant human tissue resources and laboratory models for use in endometriosis research. *Acta Obstet Gynecol Scand* 2017; **96**:644–658.
12. Xu J, Brennan TJ. Guarding pain and spontaneous activity of nociceptors after skin versus skin plus deep tissue incision. *Anesthesiology* 2010; **112**:153–164.
13. Xu J, Brennan TJ. Comparison of skin incision versus skin plus deep tissue incision on ongoing pain and spontaneous activity in dorsal horn neurons. *Pain* 2009; **144**:329–339.
14. Dolan S, Kelly JG, Monteiro AM, Nolan AM. Differential expression of central metabotropic glutamate receptor (mGluR) subtypes in a clinical model of post-surgical pain. *Pain* 2004; **110**:369–377.
15. Hains LE, Loram LC, Weiseler JL, Frank MG, Bloss EB, Sholar P, Taylor FR, Harrison JA, Martin TJ, Eisenach JC, Maier SF, Watkins LR. Pain intensity and duration can be enhanced by prior challenge: initial evidence suggestive of a role of microglial priming. *J Pain* 2010; **11**:1004–1014.
16. Gruppo Italiano per lo Studio dell'Endometriosi. Relationship between stage, site and morphological characteristics of pelvic endometriosis and pain. *Hum Reprod* 2001; **16**:2668–2671.
17. Kitawaki J, Kado N, Ishihara H, Koshiba H, Kitaoka Y, Honjo H. Endometriosis: the pathophysiology as an estrogen-dependent disease. *J Steroid Biochem Mol Biol* 2002; **83**:149–155.
18. Rižner TL. Estrogen metabolism and action in endometriosis. *Mol Cell Endocrinol* 2009; **307**:8–18.
19. Cummings AM, Metcalf JL. Induction of endometriosis in mice: a new model sensitive to estrogen. *Reprod Toxicol* 1995; **9**:233–238.
20. Bruner KL, Matrisian LM, Rodgers WH, Gorstein F, Osteen KG. Suppression of matrix metalloproteinases inhibits establishment of ectopic lesions by human endometrium in nude mice. *J Clin Invest* 1997; **99**:2851–2857.
21. Burns KA, Rodriguez KF, Hewitt SC, Janardhan KS, Young SL, Korach KS. Role of estrogen receptor signaling required for endometriosis-like lesion establishment in a mouse model. *Endocrinology* 2012; **153**:3960–3971.
22. Rajkumar K, Schott PW, Simpson CW. The rat as an animal model for endometriosis to examine recurrence of ectopic endometrial tissue after regression. *Fertil Steril* 1990; **53**:921–925.

23. Borghese B, Zondervan KT, Abrao MS, Chapron C, Vaiman D. Recent insights on the genetics and epigenetics of endometriosis. *Clin Genet* 2017; **91**:254–264.
24. Watanabe H, Numata K, Ito T, Takagi K, Matsukawa A. Innate immune response in Th1- and Th2-dominant mouse strains. *Shock* 2004; **22**:460–466.
25. Dodds KN, Staikopoulos V, Beckett EA. Uterine contractility in the non-pregnant mouse: changes during the estrous cycle and effects of chloride channel blockade. *Biol Reprod* 2015; **92**:141.
26. Cason AM, Samuelsen CL, Berkley KJ. Estrous changes in vaginal nociception in a rat model of endometriosis. *Horm Behav* 2003; **44**:123–131.
27. Clement PB. The pathology of endometriosis: a survey of the many faces of a common disease emphasizing diagnostic pitfalls and unusual and newly appreciated aspects. *Adv Anat Pathol* 2007; **14**:241–260.
28. Bergqvist A, Jeppsson S, Kullander S, Ljungberg O. Human uterine endometrium and endometriotic tissue transplanted into nude mice. Morphologic effects of various steroid hormones. *Am J Pathol* 1985; **121**:337–341.
29. Moen MH, Halvorsen TB. Histologic confirmation of endometriosis in different peritoneal lesions. *Acta Obstet Gynecol Scand* 1992; **71**:337–342.
30. Chapron C, Chopin N, Borghese B, Foulot H, Dousset B, Vacher-Lavenu MC, Vieira M, Hasan W, Bricou A. Deeply infiltrating endometriosis: pathogenetic implications of the anatomical distribution. *Hum Reprod* 2006; **21**:1839–1845.
31. Redwine DB. The distribution of endometriosis in the pelvis by age groups and fertility. *Fertil Steril* 1987; **47**:173–175.
32. Chapron C, Fauconnier A, Vieira M, Barakat H, Dousset B, Pansini V, Vacher-Lavenu MC, Dubuisson JB. Anatomical distribution of deeply infiltrating endometriosis: surgical implications and proposition for a classification. *Hum Reprod* 2003; **18**:157–161.
33. Matalliotakis IM, Cakmak H, Fragouli YG, Goumenou AG, Mahutte NG, Arici A. Epidemiological characteristics in women with and without endometriosis in the Yale series. *Arch Gynecol Obstet* 2008; **277**:389–393.
34. Vercellini P, De Giorgi O, Aimi G, Panazza S, Uglietti A, Crosignani PG. Menstrual characteristics in women with and without endometriosis. *Obstet Gynecol* 1997; **90**:264–268.
35. Lockhat FB, Emembolu JO, Konje JC. The evaluation of the effectiveness of an intrauterine-administered progestogen (levonorgestrel) in the symptomatic treatment of endometriosis and in the staging of the disease. *Hum Reprod* 2004; **19**:179–184.
36. Fortin M, Lépine M, Merlen Y, Thibeault I, Rancourt C, Gosselin D, Hugo P, Steff A-M. Quantitative assessment of human endometriotic tissue maintenance and regression in a noninvasive mouse model of endometriosis. *Mol Ther* 2004; **9**:540–547.
37. Berkley KJ, Dmitrieva N, Curtis KS, Papka RE. Innervation of ectopic endometrium in a rat model of endometriosis. *P Natl Acad Sci USA* 2004; **101**:11094–11098.
38. Peterse DP, Fassbender A, O DF, Vanhie A, Saunders P, Vriens J, Binda MM, D'Hooghe TM. Laparoscopic surgery: a new technique to induce endometriosis in a mouse model. *Reprod Sci* 2016; **23**:1332–1339.
39. McAllister SL, Dmitrieva N, Berkley KJ. Sprouted innervation into uterine transplants contributes to the development of hyperalgesia in a rat model of endometriosis. *PLoS One* 2012; **7**:e31758.
40. Mariani M, Viganò P, Gentilini D, Camisa B, Caporizzo E, Di Lucia P, Monno A, Candiani M, Somigliana E, Panina-Bordignon P. The selective vitamin D receptor agonist, elocalcitol, reduces endometriosis development in a mouse model by inhibiting peritoneal inflammation. *Hum Reprod* 2012; **27**:2010–2019.
41. Patel BG, Rudnicki M, Yu J, Shu Y, Taylor RN. Progesterone resistance in endometriosis: origins, consequences and interventions. *Acta Obstet Gynecol Scand* 2017; **96**:623–632.
42. Bruner-Tran KL, Herington JL, Duleba AJ, Taylor HS, Osteen KG. Medical management of endometriosis: emerging evidence linking inflammation to disease pathophysiology. *Minerva Ginecol* 2013; **65**:199–213.
43. Somigliana E, Vigano P, Rossi G, Carinelli S, Vignali M, Panina-Bordignon P. Endometrial ability to implant in ectopic sites can be prevented by interleukin-12 in a murine model of endometriosis. *Hum Reprod* 1999; **14**:2944–2950.
44. Herington JL, Bruner-Tran KL, Lucas JA, Osteen KG. Immune interactions in endometriosis. *Expert Rev Clin Immunol* 2011; **7**:611–626.
45. Guo SW, Du Y, Liu X. Platelet-derived TGF-beta1 mediates the down-modulation of NKG2D expression and may be responsible for impaired natural killer (NK) cytotoxicity in women with endometriosis. *Hum Reprod* 2016; **31**:1462–1474.
46. Kyama CM, Overbergh L, Debrock S, Valckx D, Vander Perre S, Meuleman C, Mihalyi A, Mwenda JM, Mathieu C, D'Hooghe TM. Increased peritoneal and endometrial gene expression of biologically relevant cytokines and growth factors during the menstrual phase in women with endometriosis. *Fertil Steril* 2006; **85**:1667–1675.
47. Kuessel L, Wenzl R, Proestling K, Balendran S, Pateisky P, Yotova Yerlikaya G, Streubel B, Husslein H. Soluble VCAM-1/soluble ICAM-1 ratio is a promising biomarker for diagnosing endometriosis. *Hum Reprod* 2017; **32**:770–779.
48. Sturlese E, Salmeri FM, Retto G, Pizzo A, De Dominici, R, Ardita FV, Borrielli I, Licata N, Laganà AS, Sofo V. Dysregulation of the Fas/FasL system in mononuclear cells recovered from peritoneal fluid of women with endometriosis. *J Reprod Immunol* 2011; **92**:74–81.
49. Christodoulakos G, Augoulea A, Lambrinoudaki I, Sioulas V, Creatsas G. Pathogenesis of endometriosis: the role of defective 'immunosurveillance'. *Eur J Contracept Reprod Health Care* 2007; **12**:194–202.
50. Panthel K, Faller G, Haas R. Colonization of C57BL/6J and BALB/c wild-type and knockout mice with Helicobacter pylori: effect of vaccination and implications for innate and acquired immunity. *Infect Immun* 2003; **71**:794–800.
51. Jiang X, Shen C, Yu H, Karunakaran KP, Brunham RC. Differences in innate immune responses correlate with differences in murine susceptibility to Chlamydia muridarum pulmonary infection. *Immunology* 2010; **129**:556–566.
52. Krzych U, Strausser HR, Bressler JP, Goldstein AL. Quantitative differences in immune responses during the various stages of the estrous cycle in female BALB/c mice. *J Immunol* 1978; **121**:1603–1605.
53. Liu L, Coller JK, Watkins LR, Somogyi AA, Hutchinson MR. Naloxone-precipitated morphine withdrawal behavior and brain IL-1beta expression: comparison of different mouse strains. *Brain Behav Immun* 2011; **25**:1223–1232.
54. Sun B, Rizzo LV, Sun SH, Chan CC, Wiggert B, Wilder RL, Caspi RR. Genetic susceptibility to experimental autoimmune uveitis involves more than a predisposition to generate a T helper-1-like or a T helper-2-like response. *J Immunol* 1997; **159**:1004–1011.
55. Freeman D, Lesche R, Kertesz N, Wang S, Li G, Gao J, Groszer M, Martinez-Diaz H, Rozengurt N, Thomas G, Liu X, Wu H. Genetic background controls tumor development in Pten-deficient mice. *Cancer Res* 2006; **66**:6492–6496.
56. Suzuki R, Kohno H, Sugie S, Nakagama H, Tanaka T. Strain differences in the susceptibility to azoxymethane and dextran sodium sulfate-induced colon carcinogenesis in mice. *Carcinogenesis* 2006; **27**:162–169.
57. Mills CD, Kincaid K, Alt JM, Heilman MJ, Hill AM. M-1/M-2 macrophages and the Th1/Th2 paradigm. *J Immunol* 2000; **164**:6166–6173.
58. Muraille E, Leo O, Moser M. Th1/Th2 paradigm extended: Macrophage polarization as an unappreciated pathogen-driven escape mechanism? *Front Immunol* 2014; **5**:603.
59. Bacci M, Capobianco A, Monno A, Cottone L, Di Puppo F, Camisa B, Mariani M, Brignole C, Ponzoni M, Ferrari S, Panina-Bordignon P, Manfredi AA et al. Macrophages are alternatively activated in patients with endometriosis and required for growth and vascularization of lesions in a mouse model of disease. *Am J Pathol* 2009; **175**:547–556.
60. Cook MJ. Viscera. In: *The Anatomy of the Laboratory Mouse*. London: Academic Press; 1965:66.